GPS total electron content variations associated with a polar cap arc

P. T. Jayachandran,[1] K. Hosokawa,[2] J. W. MacDougall,[3] S. Mushini,[1] R. B. Langley,[4] and K. Shiokawa[5]

[1]   We report an example of total electron content (TEC) variations, using Global Positioning System (GPS) measurements, associated with a polar cap arc detected by an all-sky imager and ionosonde at a polar cap station. During the transit of the arc, GPS signals along the arc length showed an increase of ∼2 TEC units whereas GPS signals perpendicular to the arc showed only an increase of ∼0.3 TEC units. This indicates that the GPS TEC variations associated with a polar cap arc are dependent on the geometry of the GPS raypaths with respect to the arc. Ionosonde measurements confirm that this arc was an E region feature at ∼110 km with peak electron density of 5.4×10^{11} el/m^3. Estimated speed of the arc using a GPS triangulation method was about 300 m/s.

Citation: Jayachandran, P. T., K. Hosokawa, J. W. MacDougall, S. Mushini, R. B. Langley, and K. Shiokawa (2009), GPS total electron content variations associated with a polar cap arc, *J. Geophys. Res.*, *114*, A12304, doi:10.1029/2009JA014916.

1.   Introduction

[2]   The polar cap ionosphere is a dynamic region and comprises different structures of ionization of varying scales sizes such as tongue of ionization, polar patches and polar cap arcs [e.g., *Tsunoda*, 1988; *Foster et al.*, 2005; *MacDougall and Jayachandran*, 2007]. Polar cap arcs are one of the most interesting and important ionospheric plasma features because of the direct implication in magnetosphere-ionosphere coupling and its link to auroral processes [e.g., *Zhu et al.*, 1997]. There are two well recognized classes of polar cap arcs [*Frank et al.*, 1986; *Valladares et al.*, 1994] linked to different intensity and energy levels of precipitation and formation mechanisms. Most of the earlier observational studies of polar cap arcs used ground-based optical measurements, radars and satellite-based optical and particle sensors. Observational and theoretical aspects of polar cap arcs were thoroughly reviewed by *Zhu et al.* [1997] and recently by *Newell et al.* [2009].

[3]   Since polar cap arcs are produced by precipitating particles [e.g., *Newell et al.*, 2009], there should be significant enhancement in the electron density in the E or F region of the ionosphere depending on the energy level of the particles. Thus an arc is a very good candidate for producing changes in the ionospheric total electron content (TEC). These TEC changes can affect the performance of the Global Positioning System (GPS) in the polar regions. We would

also like to point out that there are number of measurements from ground based radars [e.g., *Doe et al.*, 1993; *Shepherd et al.*, 1998; *Aikio et al.*, 2004] showing electron density depletions in the E and F regions associated with arcs. These depletions are produced by the upward currents in the regions closely adjacent to the arc [*Streltsov and Lotko*, 2008]. Very little is known about the TEC variations associated with polar cap arcs. In this paper, we present a case study of polar cap arc related TEC variations using GPS receivers with complementary measurements from an all-sky imager and an ionosonde located within the polar cap.

2.   Observations

[4]   For this study we have used measurements from three different instruments located at Resolute Bay (also known as Resolute) in Nunavut, Canada (74.75°N, 265.00°E geographic), a polar cap location. These three instruments are an all-sky imager, a station of the Optical Mesosphere Thermosphere Imagers (OMTIs) network [*Shiokawa et al.*, 1999; *Hosokawa et al.*, 2006], a Canadian Advanced Digital Ionosonde (CADI), and a high data rate dual-frequency GPS TEC and scintillation receiver. The CADI and GPS receiver are part of the Canadian High Arctic Ionosphereic Network (CHAIN) [*Jayachandran et al.*, 2009]. The all-sky imager measurement used for this study is the optical emission intensity at two wavelengths (630 and 557.7 nm) measured at 2 min intervals [*Shiokawa et al.*, 2009]. The GPS receivers measure ionopsheric observables at 50 Hz from which 1 min sigma phase and S4 indices are derived and range observables (pseudorange and carrier phase) at 1 Hz and the CADI records ionograms every minute and makes fixed frequency drift measurements every 30 s [*Jayachandran et al.*, 2009]. The 1 Hz GPS data was used for the results presented in this paper. The case study we are presenting here occurred between 0400 and 0600 UT on 7 November 2008. Figure 1 summarizes the observations of the arc, location of the affected GPS satellites and their

---

[1]Department of Physics, University of New Brunswick, Fredericton, New Brunswick, Canada.
[2]Department of Information and Communication Engineering, University of Electro-Communications, Chofu, Japan.
[3]Department of Physics and Astronomy, University of Western Ontario, London, Ontario, Canada.
[4]Department of Geodesy and Geomatics Engineering, University of New Brunswick, Fredericton, New Brunswick, Canada.
[5]Solar-Terrestrial Environment Laboratory, Nagoya University, Nagoya, Japan.
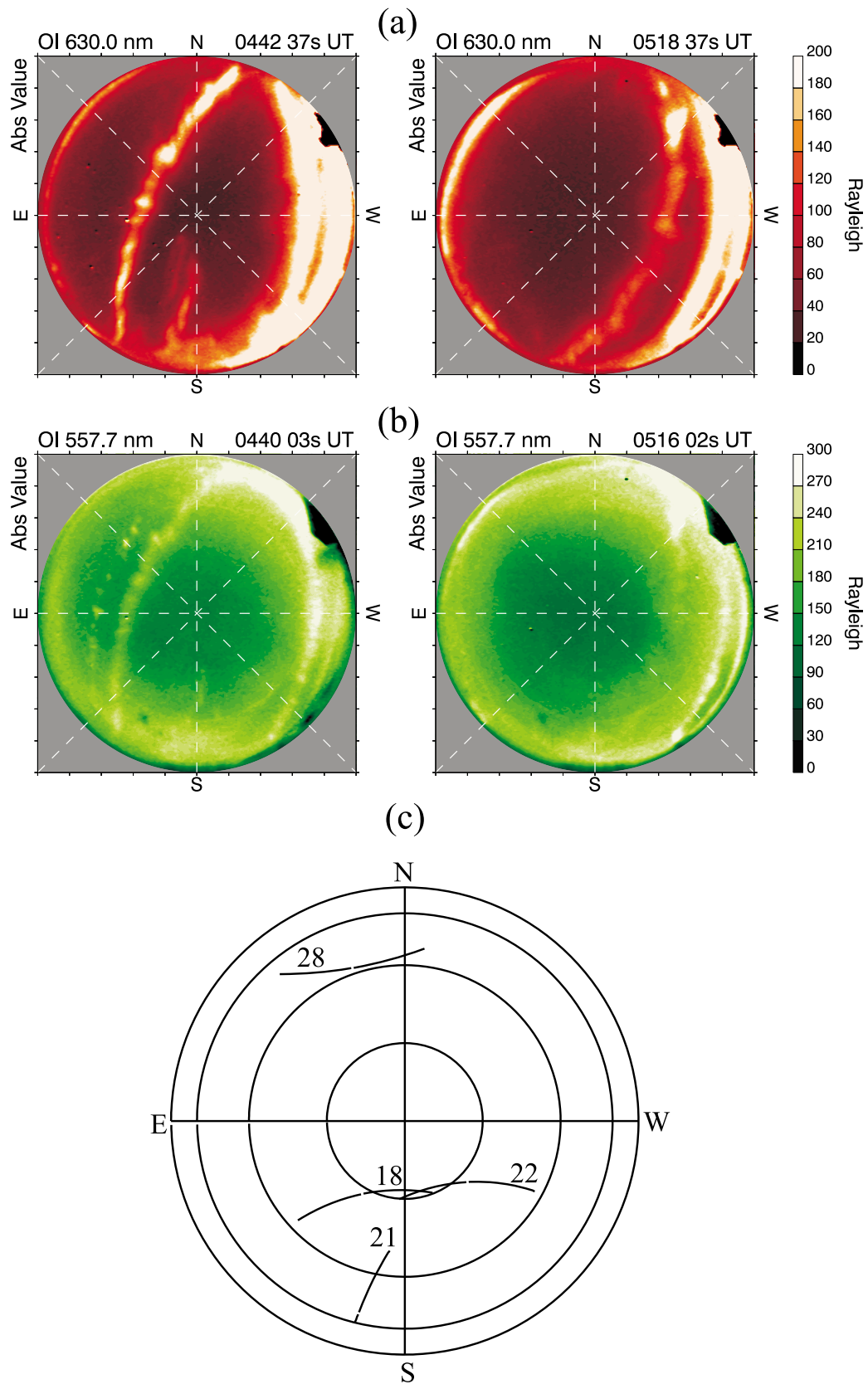
Figure 1. Resolute Bay all-sky images of (a) 630 nm at 0442 and 0518 UT, (b) 557.7 nm at 0440 and 0516 UT showing the presence of an arc on 7 November 2008. (c) Sky plot of (geographic azimuth and elevation) the four GPS satellites for the period 0400–0600 UT of 7 November 2008. Circles represents elevation angles of 0°, 10°, 30°, and 60°.
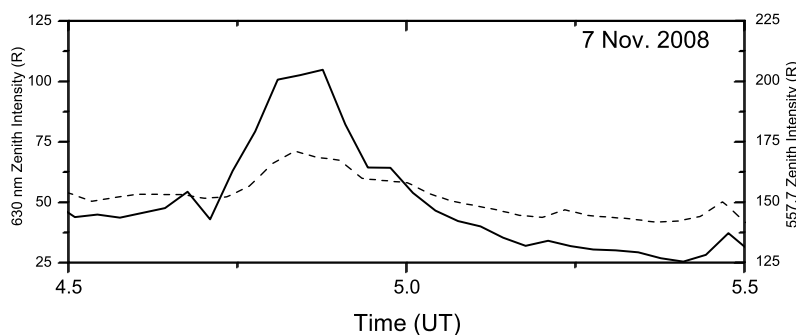
Figure 2. Zenith intensity of 630 (solid line) and 557.7 (dashed line) nm airglow emissions for the period 0430−0530 UT.

tracks during the event. Figure 1a shows two representative 630 nm all-sky images at 0242:37 and 0518:37 UT. One can see in the first image a bright arc aligned in the SE-NW direction east of the zenith and in the second image the same arc was situated west of the zenith indicating the motion of the arc. Figure 1b shows two representative 557.7 nm all-sky images and one can see the arc feature at this wavelength too. This clearly indicates that the optical feature seen in the all-sky imager is an arc. The bright optical feature seen near the western horizon of the images is the light contamination from the nearby Advanced Modular Incoherent Scatter Radar (AMISR) facility at Resolute Bay. Figure 1c shows the sky plot (azimuth and elevation) of the GPS Satellites (PRN18, PRN21, PRN22, and PRN28) for the time span 0400−0600 UT. One thing to note here, by comparing the alignment of the arc and the tracks of the GPS satellites, is that the PRN18 and PRN21 signal paths are more or less along the arc where as PRN22 and PRN 28 signal paths are across the arc.

[5] Figure 2 shows the zenith airglow intensity variations at 630 nm (solid line) and 557.7 nm (dashed line) wavelengths for the period 0430−0530 UT. It can be seen from Figure 2 that the arc reached zenith around 0450 UT indicated by the increase (∼58 R in 630 nm and ∼18 R in 557.7 nm) of the airglow emission intensity. Figure 3 shows the TEC variation along the raypaths of the four GPS satellites. The time intervals of the measurements are between 0415 and 0505 UT for PRN18, PRN21, and PRN28 and between 0440 and 0530 UT for PRN22. Figures 3a, 3b, 3c, and 3d show the variation of TEC along the raypaths of PRN 18, PRN21, PRN28, and PRN22, respectively. Relative TEC is calculated using the pseudorange and carrier phase measurements (using phase leveling-steering the pseudorange with the phase measurements in a recursive filter) and is not corrected for the instrumental biases to determine the absolute TEC values (relative variations are sufficient for the present study). One can clearly see the TEC variations of varying magnitudes associated with the passage of the arc. TEC along the PRN18 raypath shows an increase of ∼1.1 TEC units (TECU) at around 0453 UT and an increase of ∼2.1 TEC along the raypath of PRN21 around 0449 UT. TEC variations along the raypaths of PRN28 and PRN22 showed a smaller increase of ∼0.3 TECU and ∼0.6 TECU around 0456 and 0503 UT, respectively. Variation of TEC during arc on PRN 28 is suggestive because the variation is very small. The observed TEC variations are also seen in the data from a second

GPS receiver a few kilometers away, operated by Natural Resources Canada.

[6] A closer look at Figure 3 and Figure 1 reveals that the different observed increases of TEC along the different raypaths, the different times of the TEC increases, and different shapes of the TEC variations as seen from the different GPS satellites are consistent with the alignment and motion of the arc with respect to the tracks of the GPS satellites. According to scenario, the PRN18 signal will encounter the arc first, followed by PRN21 later, and then PRN22 which is the case here. Second, the PRN21 signal is aligned almost perfectly along the arc and therefore transits a longer path in the arc producing larger TEC variations (∼2 TECU). On the other hand, the PRN28 and PRN22 raypaths cross the arc and therefore experience only small TEC variations (∼0.3 TECU). This suggests that the observed TEC variations associated with the arcs are dependent on the GPS raypath geometry with respect to the arc.

3. Discussion and Conclusions

[7] We have clearly shown the existence of TEC variations associated with a polar cap arc in GPS measurements. We have also shown that the magnitude of the TEC variation depends on the geometry of the GPS raypath with respect to the arc. A previous study by *Kintner et al.* [2002] reported an increase of 10 TECU associated with an auroral arc, which is higher than the TEC variations associated with the polar cap arc reported in this paper. This is expected since in general the particle precipitation intensity in the polar cap in general is lower than that in auroral regions [e.g., *Newell et al.*, 2009]. There were no studies in the literature that we found related to TEC variations associated with polar cap arcs.

[8] The next question is whether the observed arc is an *E* region or *F* region feature. Optical measurements only confirm the presence of the arc and for the event reported in this paper, increase in the 630 nm emission intensity (∼58 R) is higher than the increase (∼18 R) in the 557.7 nm intensity. This suggests that the arc presented in this paper falls under the category of arcs produced by soft electron precipitation, which occur in the polar cap more often [*Valladares et al.*, 1994]. *Kintner et al.* [2002] used an indirect way to conclude that GPS TEC variations associated with auroral arcs are due to enhanced *E* region electron density. One direct way to answer the question is to look at ionospheric electron density measurements at the same location. Figure 4 shows ionosonde measurements
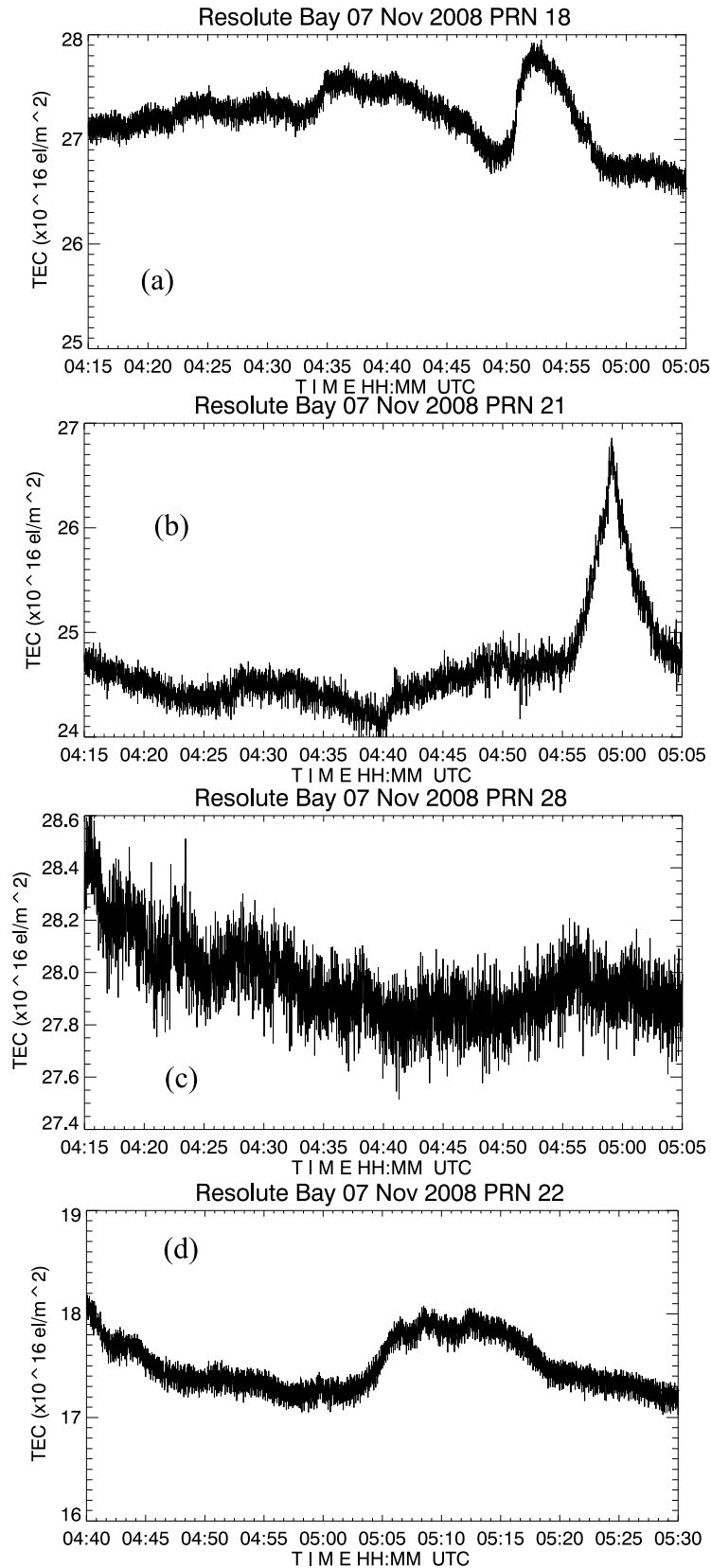
Figure 3. Variations of relative total electron content (TEC) along the raypaths of GPS satellites (a) PRN18, (b) PRN21, (c) PRN28, and (d) PRN22 for 7 November 2008 at Resolute Bay. Note that Figures 3a–3c are for the period 0415–0505 UT and Figure 3d is for the period 0440–0530 UT.
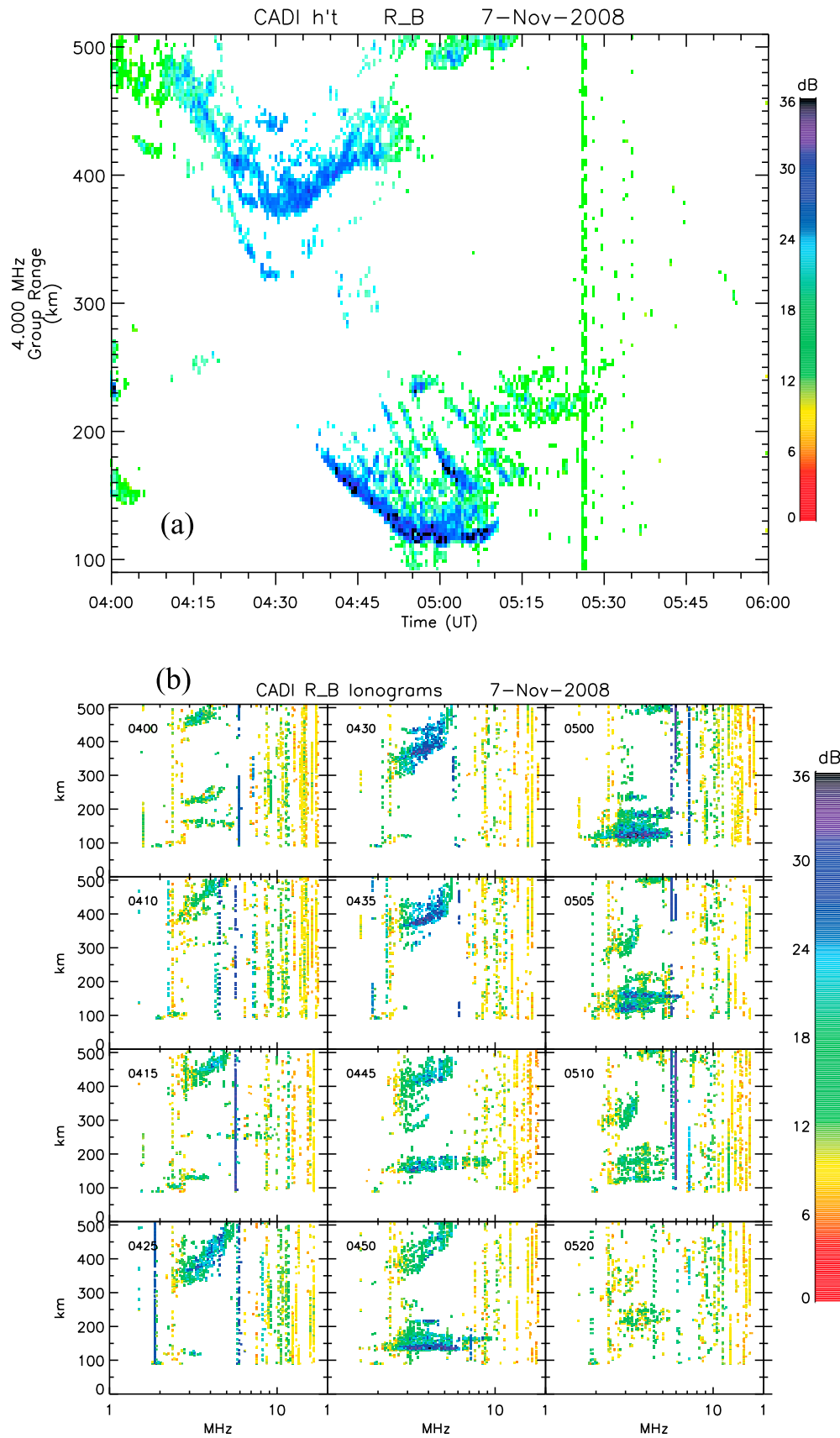
Figure 4. Resolute Bay Canadian Advanced Digital Ionosonde (CADI) (a) measurement of group range at 4 MHz for the period of 0400–0600 UT of 7 November 2008 and (b) sequence of 10 min interval ionograms between 0400 and 0520 UT.

at Resolute Bay during the event. Figure 4a shows fixed frequency (4 MHz) group range measurements using CADI for the period 0400–0600 UT, which shows the appearance of an E region feature, with a lot of structuring, around 0435 UT and the feature reached an overhead position around 0455 UT. This is consistent with the optical signatures (Figure 2) and the GPS TEC variations (Figure 3). Motion of the E region structure (a "U" shaped feature on fixed frequency group range is indicative of a moving structure) is also consistent with the all-sky imager data. Figure 4b shows a sequence of 10 min interval ionograms obtained by the CADI for the period 0400–0520 UT. A closer look at the ionograms reveals that the critical frequency of the E region structure varied between 3 and 9 MHz indicating the variation in the E region electron density. When the arc was overhead ($\sim$0455 UT) the critical frequency of the E region structure was 6.7 MHz. This corresponds to a peak electron density of $\sim$5.4 × 10^{11} el/m^3, which is a significant electron density. This directly shows that GPS TEC variations associated with the polar cap arc are due to the enhanced E region electron density. One can also estimate the equivalent vertical thickness of the arc using the ionosonde electron density and GPS TEC variations. The PRN18 raypath intersects the arc almost vertically and showed an increase of $\sim$1.1 TECU. The equivalent vertical thickness of the arc using these values is approximately 20 km.

[9] Since we have GPS TEC variations associated with the arc from multiple directions, it is possible to estimate the direction and speed of the arc using a triangulation technique. For this estimation, we have calculated the ionospheric pierce point (IPP) location of the GPS signal using a height of 110 km (the height of the arc from the ionosonde measurements) along the raypaths of the PRN18, PRN21, and PRN22 signals. Using the IPP locations and the delay of the arc signature in the TEC along these raypaths, we have estimated the arc speed and direction (IPP changes due to satellite motion are neglected in this calculation). According to this estimate, the arc was moving at a speed of $\sim$300 m/s in the direction of 52° south of west. This direction is consistent with the optical observation shown in Figure 1a. CADI also measures the drift of the ionospheric structures. Unfortunately, one of the receivers (north) was not working during the event. However, we have used the other three receivers to estimate the speed of the arc and obtained a value of $\sim$240 m/s. This value is in reasonable agreement with the speed obtained by our triangulation method (300 m/s). The arc occurred during positive interplanetary magnetic field (IMF) B_y conditions and the arc's orientation, speed, and direction of motion is consistent with the observation of *Valladares et al.* [1994] for positive IMF B_y.

References

Aikio, A. T., K. Murusula, S. Buchert, F. Forme, O. Amm, G. Marklund, M. Dunlop, D. Fontaine, A. Vaivads, and A. Fazakerley (2004), Temporal evolution of two auroral arcs as measured by the Cluster satellite and coordinated ground-based instruments, *Ann. Gephys.*, *22*, 4089–4101.

Doe, R. A., M. Mendillo, J. F. Vikrey, L. J. Zanettis, and R. W. Eastes (1993), Observation of nightside auroral cavities, *J. Geophys. Res.*, *98*, 293–310, doi:10.1029/92JA02004.

Foster, J. C., et al. (2005), Multiradar observations of the polar tongue of ionization, *J. Geophys. Res.*, *110*, A09S31, doi:10.1029/2004JA010928.

Frank, L. A., et al. (1986), The theta aurora, *J. Geophys. Res.*, *91*, 3177–3224, doi:10.1029/JA091iA03p03177.

Hosokawa, K., K. Shiokawa, Y. Otsuka, A. Nakajima, T. Ogawa, and J. D. Kelly (2006), Estimating drift velocity of polar cap patches with all-sky airglow imager at Resolute Bay, Canada, *Geophys. Res. Lett.*, *33*, L15111, doi:10.1029/2006GL026916.

Jayachandran, P. T., et al. (2009), Canadian High Arctic Ionospheric Network (CHAIN), *Radio Sci.*, *44*, RS0A03, doi:10.1029/2008RS004046.

Kintner, P. M., H. Kil, C. Deehr, and P. Schuck (2002), Simultaneous total electron content and all-sky camera measurements of an auroral arc, *J. Geophys. Res.*, *107*(A7), 1127, doi:10.1029/2001JA000110.

MacDougall, J. W., and P. T. Jayachandran (2007), Polar patches: Auroral zone precipitation effects, *J. Geophys. Res.*, *112*, A05312, doi:10.1029/2006JA011930.

Newell, P. T., K. Liou, and G. R. Wilson (2009), Polar cap particle precipitation and aurora: Review and commentary, *J. Atmos. Sol. Terr. Phys.*, *71*, 199–215, doi:10.1016/j.jastp.2008.11.004.

Shepherd, S. G., J. LaBelle, R. A. Doe, M. McCready, and A. T. Weatherwax (1998), Ionospheric structure and the generation of auroral roar, *J. Geophys. Res.*, *103*(A12), 29,253–29,266.

Shiokawa, K., Y. Katoh, M. Satoh, M. K. Ejiri, T. Ogawa, T. Nakamura, T. Tsuda, and R. H. Wiens (1999), Development of optical mesosphere thermosphere imagers (OMTI), *Earth Planets Space*, *51*(7–8), 887–896.

Shiokawa, K., Y. Otsuka, and T. Ogawa (2009), Propagation characteristics of nighttime mesospheric and thermospheric waves observed by optical mesosphere thermosphere imagers at middle and low latitudes, *Earth Planets Space*, *61*, 479–491.

Streltsov, A. V., and W. Lotko (2008), Coupling between density structures, electromagnetic waves and ionospheric feedback in the auroral zone, *J. Geophys. Res.*, *113*, A05212, doi:10.1029/2007JA012594.

Tsunoda, R. T. (1988), High latitude F region irregularities: A review and synthesis, *Rev. Geophys.*, *26*, 719–760, doi:10.1029/RG026i004p00719.

Valladares, C. E., H. C. Carlson, and K. Fukui (1994), Interplanetary magnetic field dependency of stable sun-aligned polar cap arcs, *J. Geophys. Res.*, *99*, 6247–6272, doi:10.1029/93JA03255.

Zhu, L., R. W. Schunk, and J. J. Sojka (1997), Polar cap arcs: A review, *J. Atmos. Sol. Terr. Phys.*, *59*, 1087–1126, doi:10.1016/S1364-6826(96)00113-7.

————————————

K. Hosokawa, Department of Information and Communication Engineering, University of Electro-Communications, 1-5-1 Chofugaoka, Chofu, Tokyo 182-8585, Japan.

P. T. Jayachandran and S. Mushini, Department of Physics, University of New Brunswick, P.O. Box 4400, Fredericton, NB E3B 5A3, Canada. (jaya@unb.ca)

R. B. Langley, Department of Geodesy and Geomatics Engineering, University of New Brunswick, PO Box 4400, Fredericton, NB E3B 5A3, Canada.

J. W. MacDougall, Department of Physics and Astronomy, University of Western Ontario, 1151 Richmond St., London, ON N6A 3K7, Canada.

K. Shiokawa, Solar-Terrestrial Environment Laboratory, Nagoya University, Furo-cho, Chikusa-ku, Nagoya 464-8601, Japan.